QUANTITATIVE ANALYSIS OF ELECTROMIGRATION-INDUCED DAMAGE IN Al-BASED INTERCONNECTS.

O. KRAFT, J.E. SANCHEZ, JR., and E. ARZT
Max-Planck Institut für Metallforschung, and Institut für Metallkunde, University of Stuttgart, D-7000 Stuttgart, Germany

ABSTRACT

Electromigration in metal interconnect lines produces sites of damage, such as voids, hillocks and whiskers, which by definition are the sites of flux divergence in the lines. Detailed observations of damage volume and morphology, especially in relation to the local microstructure, may yield vital information about the processes which produce the damage and ultimate failure in the interconnects. We present fractographic measurements of void volumes and the spacing between voids and corresponding hillocks in Al and Al-2% Cu interconnects which have been electromigration tested until failure. It is shown that the void density as well as the shape of failure voids depend on the current density. Further it is found that the distribution of the spacings between voids and corresponding hillocks changes as a function of current density.

INTRODUCTION

Electromigration (EM) is generally described as the net drift of metal ions due to the momentum transfer from conduction electrons which move in an applied electric field. This drift can be observed and the average drift velocity measured using, for example, the Blech edge displacement technique [1]. The effect has been attributed to mass depletion and developing tensile stresses at the cathode end and mass accumulation and developing compressive stress at the anode end of the stripe [2,3]. This stress gradient leads to a diffusional flux that counterbalances the EM mass flux. If this effect is incorporated in Black's [4] equation the following expression for the drift velocity results [1]:

$$v = \frac{D}{kT} eZ^* \rho \,(j - j_c) \qquad \text{where} \qquad j_c = \frac{\sigma^* \Omega}{eZ^* \rho \ell} \qquad (1)$$

Here D is the diffusivity (for the normally low homologous temperatures and large grains D is identical to the grain boundary diffusivity), eZ^* is the effective charge of the atom, ρ the electrical resistivity, j the current density, j_c the threshold current density, Ω the atomic volume, ℓ the length of the stripe, and σ^* the maximum hydrostatic stress the metallization is able to sustain. From equation (1) follows that below the threshold product

$$(j \cdot \ell)_c = j_c \cdot \ell = j \cdot \ell_c \le \frac{\sigma^* \Omega}{eZ^* \rho} \qquad (2)$$

no EM or stripe drift occurs.

It is common to apply this approach in understanding the effects of EM to continuous lines with near-bamboo microstructure, e.g. [5-7]. The assumed situation there is shown in Fig. 1, where the EM flux, concentrated in the grain boundaries, produces damage (i.e. voids and hillocks) at sites of flux divergence. Equation (1) suggests a direct relation between ℓ and the magnitude of the net flux along the line which produces the observable damage. It follows (equation 2) that below a certain spacing ℓ_c for a given current density no voiding should occur. Furthermore a correlation between the product $(j\ell)_c$ and the maximum stress (σ^*) is suggested, hence strengthening the film may improve EM resistance [6,8].

In this paper we apply methods of fractography, as used in the analysis of damage and failure in structural or mechanical test components, to the microstructure of EM damage in order to achieve a better understanding of the failure mechanism. We present a quantitative analysis of EM induced void size, void density and the spacing between corresponding voids and hillock in Al and Al-Cu interconnects of near bamboo microstructure. We also present the first attempts to correlate these results to existing mechanisms and models for electromigration reliability.

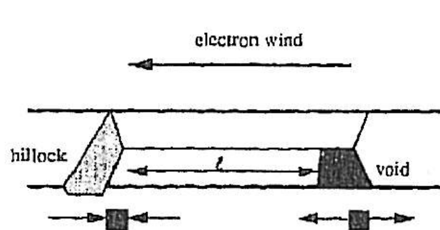

Fig. 1: Schematic illustration of the EM induced damage morphology in a continuous line, as a result of the divergences in the EM-flux.

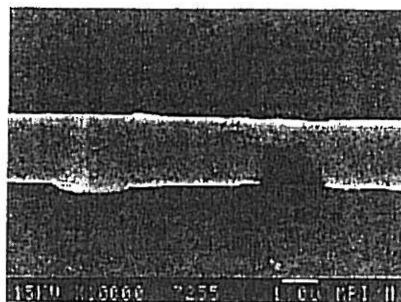

Fig. 2: SEM micrograph of a void and the corresponding hillock on an Al line.

EXPERIMENTAL PROCEDURE

Al and Al-2wt.%Cu films 0.5 μm thick were magnetron sputter deposited onto thermally oxidized (100) oriented 100 mm diameter silicon substrates. The deposition rate was approximately 2 nm/s at an Ar pressure of $2\text{-}3\cdot10^{-3}$ torr and the sputter system base pressure was better than $4.0\cdot10^{-7}$ torr. Films were annealed in forming gas in a hot wall furnace at 400°C for 45 minutes (Al) and at 425°C for 30 minutes (Al-Cu). After annealing films were patterned into parallel line arrays (PLA) of 20 lines 1 mm long (Al) or 25 lines each 1.5 mm long (Al-Cu) using standard lithographic and etch processes. Such PLA structures allow the simultaneous testing of large numbers of interconnects at a constant applied voltage with a single power supply. Failure sites will not be destroyed by arcing as the line produces an open circuit with this testing technique [9]. This method is suitable for quantitative characterization of EM induced damage.

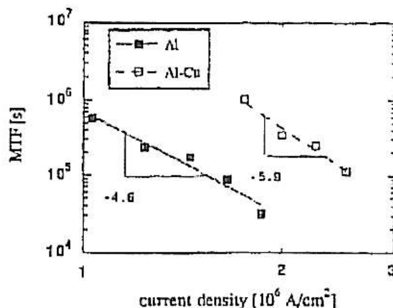

Fig. 3: A comparison of the Median Time to Failure (MTF) for the Al and the Al-Cu films as a function of current density.

The EM tests of unpassivated lines were performed on diced wafer chips placed on a hot chuck of a manual probe station. Testing temperature was 230°C, and the interconnects were 2.0 µm (Al) and 1.3 µm (Al-Cu) wide; current densities were in the ranges $1.0\text{-}1.9 \cdot 10^6$ A/cm^2 (Al) and $1.75\text{-}2.5 \cdot 10^6$ A/cm^2 (Al-Cu). The PLA resistance was constant during a stepwise increase of the current to the test condition, indicating that the line temperature was not measurably increased above the hot chuck temperature by Joule heating. After EM testing samples were observed in a scanning electron microscope (SEM). Fig. 2 shows the typical morphology observed, here a void (appearing black) and a corresponding hillock indicate the direction of current and mass flux. (In all figures the direction of the electrons is from right to left.)

The entire length of each line in the PLA was examined in the SEM for damage. A micrograph was taken of each void, and the distance to the next (downstream) hillock was measured. We assumed that the void area thus measured is directly proportional to the void volume since typically the sidewalls of the voids were perpendicular to the film surface.

RESULTS

Results of EM testing for the two films are shown in fig. 3: the dependence of Median Time to Failure (MTF) on the current density is given by the well established relation MTF ~ j^{-n}, where the current exponents (n) are 4.6 (Al) and 5.9 (Al-Cu). These values are higher than the often reported value of 2.

The SEM observations of the tested structures clearly reveal differences in the extent of EM damage between films and current densities. Void density, defined as the total number of voids divided by the entire length of interconnects in the PLA circuit, is shown in figure 4a. The increase of void density with current density is due to a greater number of voids at all spacings, to be discussed below.

The „length" (measured in the direction along the line) of voids responsible for failure is determined as follows. By definition a fatal void must cross the linewidth (W). In order to compare fatal void geometries or sizes in lines of different widths the measured void area (A_v) is normalized by W, which is 2.0 µm and 1.3 µm in the Al and Al-Cu interconnects, respectively. The resulting measure of the fatal void size is shown in figure 5a, where each plotted value is an average of 20 (Al) or 25 (Al-Cu) fatal voids. We note a possible trend of decreasing void length above approximately $1.8 \cdot 10^6$ A/cm^2 for the Al and above $2.3 \cdot 10^6$ A/cm^2 for the Al-Cu interconnects. Such a trend would suggest a change in the void growth mechanism, which is particularly obvious when the Al and Al-Cu data are combined.

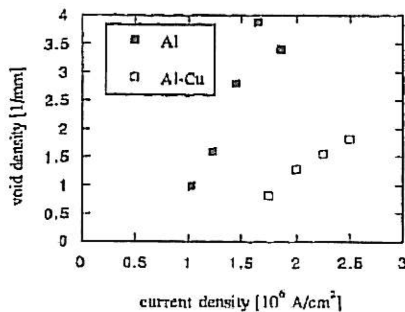

Fig. 4a: Void densities of both films Al and Al-Cu as a function of applied current density.

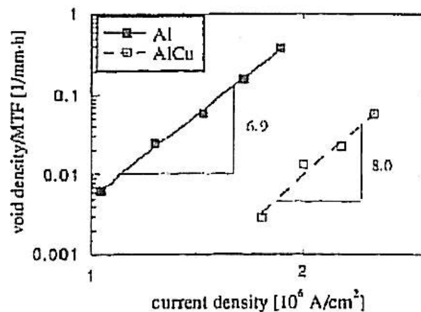

Fig. 4b: Average void nucleation rate as determined by dividing void density by MTF of each test.

For both films and all test conditions the measured spacings are lognormally distributed, as shown in figure 6a for the Al film at two extreme current densities. It is seen that the median as well as the minimum spacings decrease as the applied current increases. Preliminary analysis suggests that the minimum spacing ℓ_{min} decreases proportional to j^{-3}, which is a stronger dependency than it would be expected from equation (2). The threshold product $(j\ell)_c$ is shown in figure 6b as a function of the current density. Here the minimum spacing ℓ_{min} found in each test was used to calculate the threshold product: $(j\ell)_c = j \cdot \ell_{min}$. The threshold product is shown to decrease with j for both Al and Al-Cu, whereas the absolute values of the threshold products are higher for the Al-Cu film compared to the Al film.

DISCUSSION

The dependence of MTF on the current density shown in figure 3 is stronger than expected. Such high current exponents often occur when a high current density produces Joule heating in the interconnect. However, we can practically rule out this possibility, since a resistance increase was not detected and voids and hillocks were randomly distributed over the entire line length. The reason for the high current exponent is at present unclear.

The void density, as measured after failure of the last line, increases characteristically with current density (fig. 4a). By analyzing the data of spacings between voids and hillocks it turns out that this is due to the decrease of the minimum spacing ℓ_{min} as well as an increase of the number of void-hillock pairs with larger spacings. Because the test duration decreased with increasing current density, it makes sense to divide the void density by the MTF at that particular current density; in this way an approximate „average void nucleation rate“ is obtained (fig. 4b), which exhibits a strong power-law dependence on j. (Note that even the somewhat inconsistent last data point for Al in fig. 4a now conforms to the straight line fig. 4b). It is also instructive that void nucleation is approximately two orders of magnitude slower in Al-Cu.

A similiar normalization with respect to MTF can be carried out for the average void area (fig. 5b). Because of the expected continuous void nucleation, however, the resulting „average void growth rates“ must be considered as rough approximations. It is seen that again a power-law

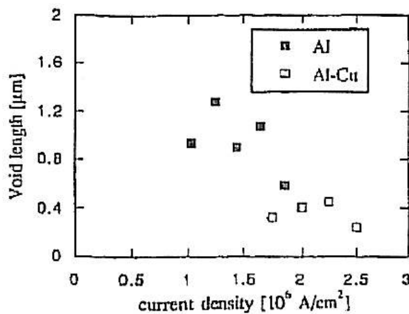

Fig. 5a: Void length defined as measured void area A_V divided by the width W of the line.

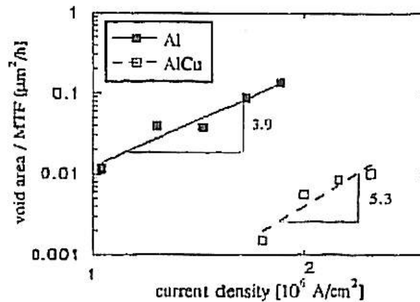

Fig. 5b: Estimate of the average void growth rate obtained by dividing the measured void area A_V by MTF of each test.

behaviour obtains and that Cu slows down void growth by two orders of magnitude. The current exponent, while greater than 1 (the value expected on the basis of equation (1)), is characteristically smaller than that for the void nucleation rate.

The determined threshold products $(j\ell)_c$ for both films have the same order of magnitude as found by others using the edge displacement method [1, 10]. However, it is inconsistent with the simple Blech model that the threshold product depends on the current density. Further the results suggest that the Al-Cu film is about six times stronger than the Al film. This is not consistent with recent results by R. Venkatraman [11], who has shown that continuous Al and Al-Cu films have about the same mechanical properties as determined using the wafer curvature technique. Measurements of the strength of interconnects are necessary to test this result for isolated lines.

An observation which is significant for future modelling of the damage accumulation is contained in fig. 5a. The decrease in „length" of the fatal void characterizes a trend which has been qualitatively observed on micrographs: with increasing current density, less material has to be moved by EM and the failure void becomes increasingly more „slit-like". There is an interesting analogy to this situation in creep-failure of high-temperature materials, e.g. [12]. Grain boundary

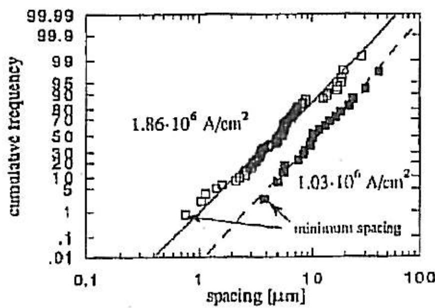

Fig. 6a: Distributions of spacings between voids and corresponding hillocks after EM testing of the Al film at two different current densities.

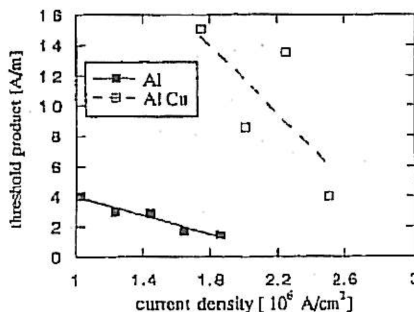

Fig. 6b: Dependence of the threshold product $(j\ell)_c$ on the current density for both films.

voids which grow under the action of a tensile stress maintain a spherical equilibrium shape only if surface diffusion is more rapid than grain-boundary diffusion; if on the other hand void growth is controlled by (slow) surface diffusion, voids grow in a crack-like manner. Further analysis and additional tests at higher current densities are presently being performed to verify this mechanism in electromigration.

CONCLUSIONS

As a result of quantitative characterization of EM induced damage the following conclusions can be made:

1. The void density increases with current density due to both a decrease in the minimum void-hillock spacing and an increase in number of voids at all spacings. When the void density is normalized by MTF, an approximate „void nucleation rate" can be obtained which varies strongly with current density.
2. We find an apparent void size decrease above a current density of $1.8 \cdot 10^6$ A/cm^2 for Al and $2.3 \cdot 10^6$ A/cm^2 for Al-Cu. This corresponds to a qualitative trend to a greater frequency of slit like voids at higher current densities. A possible reason for this transition is a change of the rate-controlling diffusion mechanism.
3. The threshold product $(j\ell)_c$ has been found to lie in the range between 200 and 1200 A/cm, roughly the same order of magnitude as in other studies. However we find that the critical product decreases with increasing current for both Al and Al-Cu.
4. Careful observation of EM induced damage may yield information about microscopic mechanisms for void and hillock formation which should be helpful for further modelling.

ACKNOWLEDGEMENTS

We acknowledge helpful discussions with Dr. J. Lloyd. We are also grateful to Dr. S. Bader and Prof. W.D. Nix for an ongoing collaboration Stanford-Stuttgart, which is supported by the Humboldt Foundation and the Max-Planck-Society in the form of a Max-Planck Research Award.

REFERENCES

1. I.A. Blech, J. Appl. Phys. 47, 1203 (1976)
2. I.A. Blech and C. Herring, Appl.Phys. Lett. 29, 131 (1976)
3. I.A. Blech and K.L. Tai, Appl.Phys. Lett 30, 387 (1977)
4. J.R. Black, IEEE Trans. Electr. Dev. 16, 338 (1969)
5. M. Shatzkes and J.R. Lloyd, J. Appl. Phys. 59, 3890 (1986)
6. E. Arzt and W.D. Nix, J. Mat. Res. 6, 731 (1991)
7. C.A. Ross, Mat. Res. Soc. Proc. 225, 35 (1991)
8. E. Arzt, O. Kraft, J. Sanchez, S. Bader and W.D. Nix, Mat. Res. Soc. Proc."Thin Films: Stresses and Mecanical Properties III" (1991)
9. J.E. Sanchez Jr., L.T. McKnelly and J.W. Morris Jr., J. El. Mat. 19, 1213 (1990)
10. C.A. Ross, J.S. Drewery, R.E. Somekh and J.E. Evett, J. Appl. Phys. 66, 2349 (1989)
11. R. Venkatraman and J.C. Bravman, Mat. Res. Soc. Proc."Thin Films: Stresses and Mecanical Properties III" (1991)
12. A.C.F. Cocks and M.F. Ashby, Progr. Mat. Sci.17, 189 (1982)